

## Design, Parallel Synthesis, and Crystal Structures of Pyrazinone Antithrombotics as Selective Inhibitors of the Tissue Factor VIIa Complex

John J. Parlow,<sup>\*,†</sup> Brenda L. Case,<sup>†</sup> Thomas A. Dice,<sup>†</sup> Ricky L. Fenton,<sup>†</sup> Michael J. Hayes,<sup>†</sup> Darin E. Jones,<sup>†</sup> William L. Neumann,<sup>†</sup> Rhonda S. Wood,<sup>†</sup> Rhonda M. Lachance,<sup>‡</sup> Thomas J. Girard,<sup>‡</sup> Nancy S. Nicholson,<sup>§</sup> Michael Clare,<sup>||</sup> Roderick A. Stegeman,<sup>⊥</sup> Anna M. Stevens,<sup>⊥</sup> William C. Stallings,<sup>⊥</sup> Ravi G. Kurumbail,<sup>⊥</sup> and Michael S. South<sup>†</sup>

Department of Medicinal and Combinatorial Chemistry, Pharmacia Corporation, 800 North Lindbergh Boulevard, St. Louis, Missouri 63167, Department of Cardiovascular and Metabolic Disease, Pharmacia Corporation, 800 North Lindbergh Blvd., St. Louis, Missouri 63167, Department of Cardiovascular Pharmacology, Pharmacia Corporation, 4901 Searle Parkway, Skokie, Illinois 60077, Structure and Computational Chemistry, Pharmacia Corporation, 4901 Searle Parkway, Skokie, Illinois 60077, and Structure and Computational Chemistry, Pharmacia Corporation, 700 Chesterfield Village Parkway, St. Louis, Missouri 63198

Received March 20, 2003

Structure-based drug design (SBDD) and polymer-assisted solution-phase (PASP) library synthesis were used to develop a series of pyrazinone inhibitors of the Tissue Factor/Factor VIIa (TF/VIIa) complex. The crystal structure of a tripeptide- $\alpha$ -ketothiazole complexed with TF/VIIa was utilized in a docking experiment to identify the pyrazinone core as a starting scaffold. The pyrazinone core could orient the substituents in the correct spatial arrangement to probe the S<sub>1</sub>, S<sub>2</sub>, and S<sub>3</sub> pockets of the enzyme. A multistep PASP library synthesis was designed to prepare the substituted pyrazinones varying the P<sub>1</sub>, P<sub>2</sub>, and P<sub>3</sub> moieties. Hundreds of pyrazinone TF/VIIa inhibitors were prepared and tested in several serine protease enzyme assays involved in the coagulation cascade. The inhibitors exhibited modest activity on TF/VIIa with excellent selectivity over thrombin (IIa) and Factor Xa. The structure–activity relationship of the pyrazinone inhibitors will be discussed and X-ray crystal structures of selected compounds complexed with the TF/VIIa enzyme will be described. This study ultimately led to the synthesis of compound **34**, which exhibited 16 nM (IC<sub>50</sub>) activity on TF/VIIa with >6250 $\times$  selectivity vs Factor Xa and thrombin. This potent and highly selective inhibitor of TF/VIIa was chosen for preclinical, intravenous proof-of-concept studies to demonstrate the separation between antithrombotic efficacy and bleeding side effects in a nonhuman primate model of electrolytic-induced arterial thrombosis.

### Introduction

Blood coagulation is initiated upon vascular injury when plasma Factor VIIa comes in contact with its essential cofactor, Tissue Factor (TF), which is an integral membrane protein not normally in contact with blood. The TF/VIIa complex proteolytically activates its substrates, Factors IX and X. This triggers a cascade of reactions, ultimately resulting in the generation of thrombin and a fibrin clot.<sup>1–10</sup> Disruption of atherosclerotic plaques, and the subsequent release of plasma factor VIIa leading to occlusive thrombus formation, is the main cause of the acute syndromes of unstable angina, myocardial infarction, and sudden death.<sup>11,12</sup> Effective and safe antithrombotics are needed to combat these diseases. Most research has focused on thrombin and Factor Xa inhibitors as potentially valuable therapeutic agents for these diseases.<sup>13–18</sup> Since TF/VIIa triggers the thrombotic process, this complex is a prime target for intervention in these vascular diseases. Recently, small molecule inhibitors of TF/VIIa have

been the subject of intense research because of their potential to inhibit the coagulation cascade.<sup>19–32</sup> There is evidence from our own laboratories, as well as others, that selective inhibition of the TF/VIIa complex may provide effective anticoagulation while lessening the risk of the bleeding side effects associated with other antithrombotic mechanisms, such as glycoprotein IIb/IIIa antagonists and inhibitors of Factor Xa and thrombin.<sup>33–36</sup> Therefore, structure-based drug design (SBDD) and parallel medicinal chemistry were used to develop a series of potent and selective TF/VIIa inhibitors to address the large, unmet medical need for safe and effective oral anticoagulants.

We recently described the synthesis and structure–activity relationship (SAR) of a series of tripeptide- $\alpha$ -ketothiazoles.<sup>37,38</sup> These reversible, covalent, serine protease inhibitors had nanomolar potency against TF/VIIa and exhibited 500 $\times$  selectivity vs thrombin (Figure 1). This study demonstrated that it is possible to achieve potent inhibition of the TF/VIIa complex while maintaining selectivity against other highly homologous serine proteases in the coagulation cascade. Several reports of small molecule TF/VIIa inhibitors have appeared, with varying degrees of selectivity vs the other plasma proteases in the coagulation cascade.<sup>19,21,22,24,25,29</sup> We hypothesized that a wider selectivity margin over

\* To whom correspondence should be addressed. Phone: 314-274-3494. Fax: 314-274-1621. e-mail: john.j.parlow@pfizer.com.

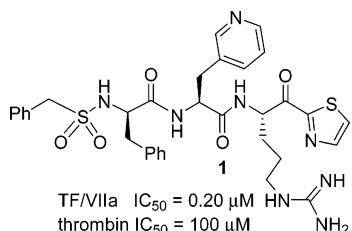
<sup>†</sup> Department of Medicinal and Combinatorial Chemistry.

<sup>‡</sup> Department of Cardiovascular and Metabolic Disease.

<sup>§</sup> Department of Cardiovascular Pharmacology.

<sup>||</sup> Structure and Computational Chemistry.

<sup>⊥</sup> Structure and Computational Chemistry.

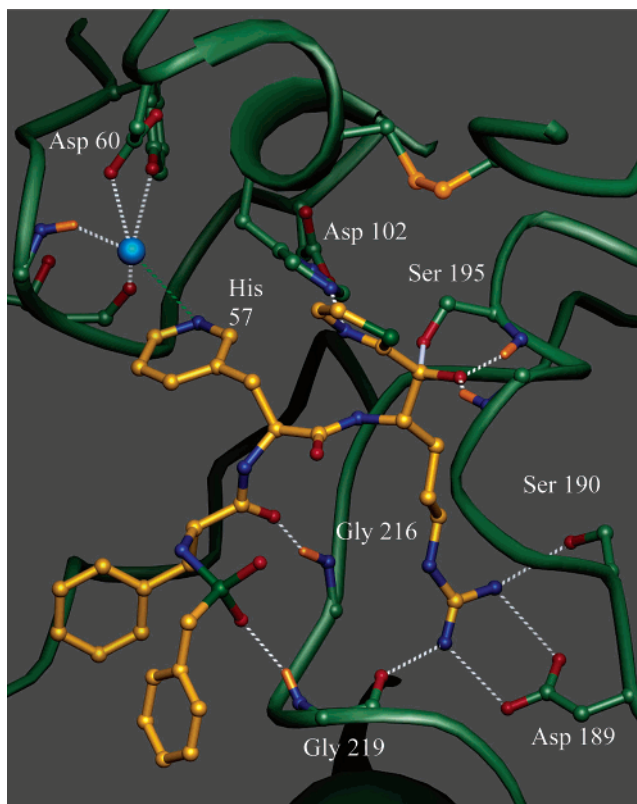


**Figure 1.** Ketothiazole TF/VIIa inhibitor.

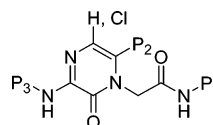
Factor Xa and thrombin was necessary to unequivocally demonstrate that inhibition of TF/VIIa would lead to a lower bleeding side effect relative to that observed with Factor Xa and thrombin inhibitors. These highly selective TF/VIIa inhibitors should then be suitable for preclinical, intravenous proof-of-concept studies demonstrating the separation between antithrombotic efficacy and bleeding side effects in a primate model of thrombosis.<sup>39</sup> The structural information obtained from the tripeptide- $\alpha$ -ketothiazoles bound to TF/VIIa, combined with the crystal structure of other related serine proteases such as thrombin and Factor Xa, facilitated the development of a series of highly selective, small molecule inhibitors of TF/VIIa that were nonpeptidic and did not interact with the catalytic apparatus of the enzyme.<sup>40,41</sup> Herein, we report the progression from a peptidic lead to the development of noncovalent, highly selective small molecule inhibitors of the TF/VIIa complex utilizing SBDD coupled with PASP library synthesis.<sup>42</sup> The structure–activity relationship will be discussed, and X-ray crystal structures of selected compounds complexed with the TF/VIIa enzyme will be described.

## Results and Discussion

Information obtained from various crystal structures of TF/VIIa,<sup>37,38,43–46</sup> thrombin,<sup>47,48</sup> and Factor Xa<sup>49–53</sup> was used to develop the initial small molecule inhibitors of TF/VIIa. The X-ray crystal structure of the tripeptide- $\alpha$ -ketothiazole **1** bound to the TF/VIIa enzyme is shown in Figure 2. Excluding the catalytic apparatus, several key interactions were crucial for both potency and selectivity over thrombin and Factor Xa. The arginine side chain at P<sub>1</sub> forms four strong hydrogen bonds at the bottom of the S<sub>1</sub> pocket with the side chains of Asp 189 and Ser 190 as well as to the backbone carbonyl oxygen of Gly 219. The inhibitor forms two other hydrogen bonds with the peptide nitrogens of Gly 216 and Gly 219. The S<sub>2</sub> pocket of Factor VIIa is relatively open and has a negative potential due to the presence of Asp 60. The pyridyl group of the inhibitor takes advantage of these structural features to form strong interactions in the S<sub>2</sub> pocket of VIIa. Among the coagulation proteases, only Factor VIIa has a negatively charged residue at position 60. In contrast, Factor Xa has a tyrosine at position 60. Moreover, the S<sub>2</sub> pocket of Factor Xa is occluded by the side chain of Tyr 99. Thrombin has a large insertion in the S<sub>2</sub> pocket with a number of aromatic amino acid residues. These structural differences account for the enhanced selectivity of compound **1** for TF/VIIa over thrombin and Factor Xa. It was theorized that the ketothiazole moiety was contributing to a loss of selectivity, since this moiety captures the catalytic apparatus of all of the homologous



**Figure 2.** Crystal structure of ketothiazole **1** bound in the active site of TF/VIIa complex. Some of the key side chains of Factor VIIa are displayed (C: green, N: dark blue, O: red, S: yellow, H: orange). The inhibitor is represented with carbon, nitrogen, oxygen, and sulfur atoms displayed in yellow, blue, red, and green, respectively. The hydrogen bonds formed by the inhibitor and a bound water molecule in the S<sub>2</sub> site are shown as dotted white lines. The close interaction between the bound solvent and the pyridyl nitrogen of the inhibitor is shown as a dotted green line. The active site serine, Ser 195, forms a covalent bond, shown as a thin solid line, with the activated carbon of the inhibitor.

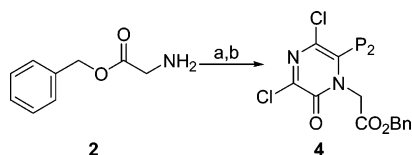


**Figure 3.** Pyrazinone core structure.

serine proteases. As a result, the intended inhibitors were designed such that they did not interact with the catalytic apparatus.

Using these key features of the TF/VIIa crystal structure, a series of six-membered heterocyclic cores were docked, which led to the pyrazinone scaffold as a prototype inhibitor to begin our SBDD studies (Figure 3). The pyrazinone core orients the substituents in the correct spatial arrangement to probe the S<sub>1</sub>, S<sub>2</sub>, and S<sub>3</sub> pockets of the enzyme. In addition, the NH of the P<sub>3</sub>, the NH of the glycine, and the carbonyl of the pyrazinone core provide potential hydrogen bonds to the peptide backbone of the enzyme. The pyrazinone core had previously been used in the design of inhibitors for thrombin<sup>54–58</sup> and is bound in the enzyme in a similar fashion.

Several pyrazinone cores were prepared according to a literature procedure to provide building blocks for library synthesis.<sup>50,51,53,54</sup> The synthesis involved a

**Scheme 1.** Pyrazinone Core Structure Synthesis<sup>a</sup>

<sup>a</sup> Reagents: (a) TMSCN, P<sub>2</sub>CHO 3, CH<sub>2</sub>Cl<sub>2</sub>; (b) (ClCO)<sub>2</sub>, 1,2-dichlorobenzene.

modified Strecker reaction between glycine benzyl ester 2, trimethylsilylcyanide, and an aldehyde 3, followed by cyclization of the intermediate with oxalyl chloride to give the desired dichloropyrazinone 4 (Scheme 1). The P<sub>2</sub> diversity element was contained in the starting aldehyde and thus was hardwired in place at the beginning of the synthesis. The aldehyde inputs were biased such that the final products would mimic the phenylalanine P<sub>2</sub> analogues of the ketothiazole series.

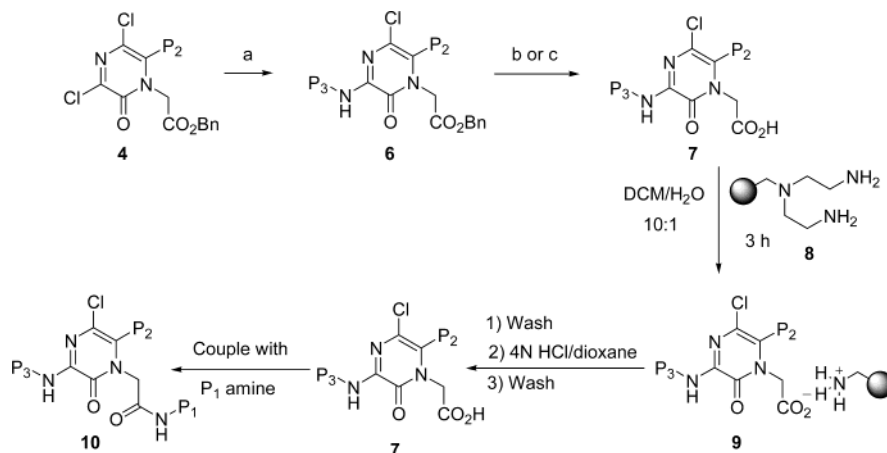
In an effort to rapidly prepare libraries of pyrazinones in a parallel format, a solution-phase library synthesis was developed using PASP technology.<sup>61–63</sup> A summary description of the library synthesis is depicted in Scheme 2. The goal of the library synthesis was to use the PASP synthesis technology in such a way as to eliminate the need for chromatography and isolation of intermediates. The synthesis was accomplished using a combination of polymeric reagents and PASP purification concepts, including reactant-sequestering resins and resin capture-release. To maximize the efficiency of the multistep sequence and to minimize manual manipulation of the reaction vessels, multiple reaction steps were carried out in the same vessel. Each of the steps in the synthesis underwent independent validation to identify and optimize conditions such that each transformation could be performed in a high-yielding, parallel format. The synthesis is general and variations of both the P<sub>3</sub> and P<sub>1</sub> inputs are easily allowed.

The first step of the synthesis was a nucleophilic displacement of the 3-chloro of pyrazinone 4 with the desired P<sub>3</sub> amine 5. In the initial validation studies, *N*-methylmorpholine was used as the base and dimethylformamide was used as the solvent. Byproducts resulting from addition of morpholine and dimethylamine at the P<sub>3</sub> position were observed. Using excess P<sub>3</sub> amine 5 (3 equiv) as both reactant and base and using acetonitrile as the solvent at 70 °C overnight

afforded desired products 6. Rather than purify at this step, the crude reaction mixture was carried on to the next step.

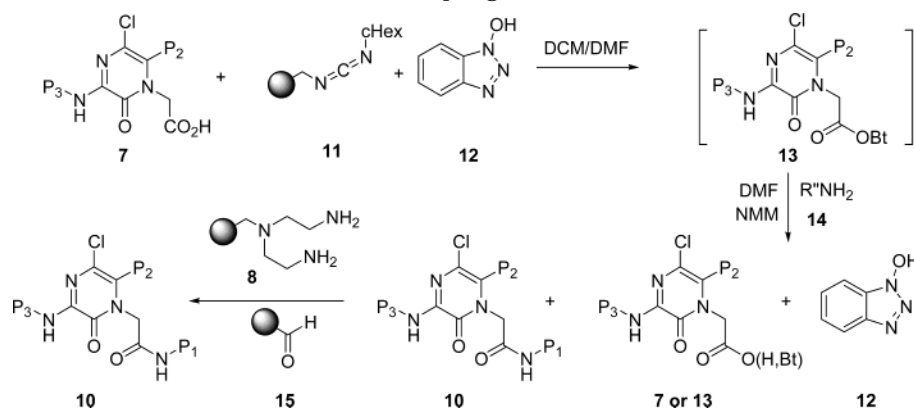
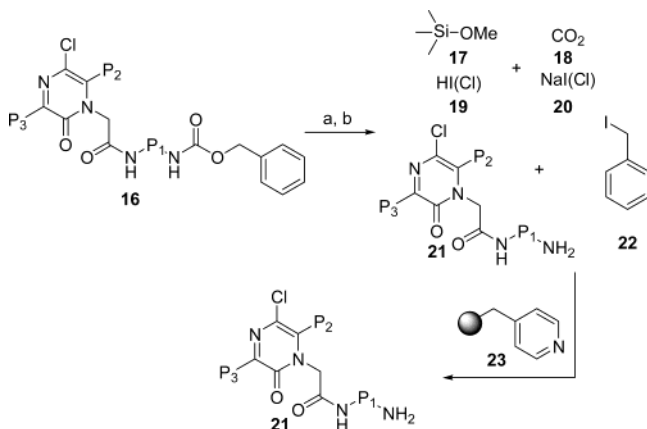
The second step of the synthesis involved a series of manipulations in the same reaction vessel. The benzyl ester 6 was hydrolyzed by adding a solution of potassium hydroxide in methanol to each reaction vessel. Upon completion of hydrolysis, the reaction mixture was acidified with 4 N hydrochloric acid in dioxane and then evaporated to dryness. Alternatively, when the P<sub>2</sub> phenyl ring contained an ester functionality, the pyrazinone 6 was treated with hydrogen and palladium on carbon to remove the benzyl ester. In the initial studies, the resulting pyrazinone carboxylic acid was captured onto polycarbonate resin. However, this resulted in significant formation of byproducts. Polyamine resin 8 successfully captured the pyrazinone carboxylic acid intermediate without causing the formation of the byproducts. Each mixture was then poured directly onto a disposable filter, and the product-containing resin 9 was washed sequentially with a variety of solvents to remove the benzyl alcohol, amine hydrochloride, potassium chloride, and other impurities that were present. The resin was dried and the acids were released from the resin with 4 N hydrochloric acid in dioxane. The pyrazinone carboxylic acid intermediates 7 were obtained in pure form after filtration and evaporation.

The next step of the synthesis incorporated the P<sub>1</sub> input on the pyrazinone through an amide coupling (Scheme 3). The pyrazinone acids 7 were incubated at room temperature with the polymer-bound carbodiimide 11 and hydroxybenzotriazole 12 to afford the activated 1-hydroxybenzotriazole esters 13. The amine 14 and a 3-fold stoichiometric excess of *N*-methylmorpholine were added to each reaction vessel to afford products 10. Upon completion of the reaction, a mixed-resin bed of the polyamine resin 8 and aldehyde resin 15 was added to each reaction vessel to sequester the hydroxybenzotriazole 12, remaining activated ester 13, and any unreacted acid 7 or amine 14. The sequestering resins were agitated for a period of 2 h. If an incubation time of an extended period was used, a chloromethyl adduct of 1-hydroxybenzotriazole was observed as an impurity.<sup>64,65</sup> Simple filtration and rinsing with dichloromethane and dimethylformamide, followed by evapo-

**Scheme 2.** Polymer-Assisted Solution-Phase (PASP) Pyrazinone Synthesis<sup>a</sup>

<sup>a</sup> Reagents: (a) 3 equiv of P<sub>3</sub>NH<sub>2</sub> 5, AcCN (b) (i) aq KOH, MeOH; (ii) 4 N HCl/dioxane; (c) H<sub>2</sub>, Pd/C.



**Scheme 3.** Polymer-Assisted Solution-Phase (PASP) Coupling of P<sub>1</sub> Amine**Scheme 4.** CBz Deprotection Protocol<sup>a</sup>

<sup>a</sup> Reagents: (a) TMSCl, NaI, acetonitrile; (b) MeOH.

ration of the solvents, afforded pure products **10** from each parallel reaction.

The P<sub>1</sub> amine inputs **14** were biased toward containing a basic moiety to engage the Asp 189. As a result, many of the basic groups of the P<sub>1</sub> amines **14** were protected with either a BOC or CBz protecting group. The BOC protecting group was easily removed by incubating the compound with 4 N hydrochloric acid in dioxane, followed by evaporation to afford the desired products. Two deprotection protocols could be used for removal of the CBz group. The use of high-pressure hydrogen with palladium on carbon resulted in both the deprotection of the CBz group and the reduction of the chloro at the 5-position to give 5-hydropyrazinone analogues. The reductions were run in parallel using an Argonaut Endeavor reactor. A second deprotection protocol for the CBz protecting group was required which allowed the chlorine to remain intact and the reaction to be run in a parallel format using PASP technology. In a modified solution-phase procedure that generated trimethylsilyl iodide in situ,<sup>66</sup> the CBz group was removed by heating an acetonitrile solution of compound **16** in the presence of excess sodium iodide and trimethylsilyl chloride to afford product **21** (Scheme 4). The reaction was quenched with methanol to give volatile byproducts **17**, **18**, and **19**. Polyvinyl pyridine **23** was then added to sequester the benzyl iodide byproduct **22**. The polymer-bound benzyl iodide **22** was filtered away along with the NaI(Cl) **20**, the only other nonvolatile byproduct generated in the reaction. It should be noted that when a polymer-bound primary

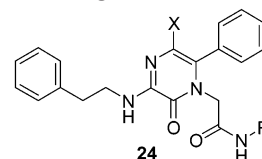
or secondary amine was used as a sequestering resin with products that contained an amidine group, the resin reacted with the amidine group and sequestered the desired product.

Several hundred compounds were prepared from the synthesis described above. All of the inhibitors were screened against several serine protease enzymes involved in the coagulation cascade, including TF/VIIa, thrombin (IIa), and Factor Xa. Each enzyme assay consisted of the specific enzyme and the chromogenic substrate for that enzyme. Reported are the inhibition data as IC<sub>50</sub> values for TF/VIIa and thrombin. In general, these compounds were selective vs Factor Xa with no activity observed at concentrations of 30 μM and/or 100 μM. Factor Xa has a tyrosine at position 60, and the S<sub>2</sub> pocket of Factor Xa is occluded by the side chain of Tyr 99. Thus, selectivity vs Factor Xa is probably due to a collision of the P<sub>2</sub> phenyl ring with the Tyr 99 of Factor Xa (data not shown).

The structure–activity relationships of the pyrazinone series can be divided into three parts: the amidine which occupies the S<sub>1</sub> pocket and interacts with Asp 189, the 3-amino substituent that occupies the S<sub>3</sub> pocket, and the substituent at the 6-position that occupies the S<sub>2</sub> pocket (Figure 3). Chemistry efforts exploring all three points of diversification occurred simultaneously in the lab. Described first is the progress and structure–activity relationships around S<sub>1</sub>, followed by S<sub>3</sub>, and concluding with the S<sub>2</sub> pocket.

Early in the program, libraries with P<sub>1</sub> inputs containing various basic or hydrogen bond-accepting groups were prepared in an attempt to engage the Asp 189 at the bottom of the S<sub>1</sub> pocket. A representative sample of analogues with various P<sub>1</sub> amides is shown in Table 1. Data from the first set of compounds established that *p*-benzamidine as the P<sub>1</sub> amide was required for any type of biological activity (**24a,b**).<sup>67</sup> All other analogues, including compounds containing *p*-phenethylamidine **24e** or *m*-benzamidine **24f**, were inactive. Replacing the *p*-benzamidine with either pyridylamidine regioisomer, compounds **24c** and **24d**, resulted in a loss of potency on TF/VIIa.<sup>68</sup>

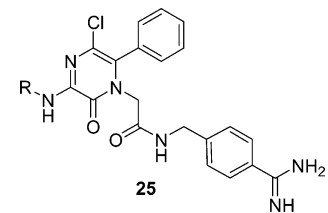
It was determined early in the project that *p*-benzamidine as the P<sub>1</sub> moiety was crucial for potency. Thus, chemistry efforts focused primarily on exploring the P<sub>2</sub> and P<sub>3</sub> groups. On the basis of crystal structure data, the S<sub>3</sub> pocket is wide-open and hydrophobic with residues Val 170E, Pro 170I, and Gln 217 from the peptide segment. Initially, potential inhibitors with relatively

**Table 1.** Pyrazinone Analogs with Various P<sub>1</sub> Amides


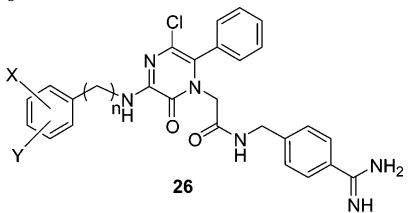
Cpd	R	X	IC <sub>50</sub> (μM)	
			VIIa	IIa
24				
a		Cl	0.63	0.16
b		H	0.34	0.30
c		H	16.7	3.1
d		H	1.4	0.15
e		H	>30	>30
f		H	>30	>30
g		Cl	>100	>100
h		Cl	>100	>100
i		Cl	>100	>100
j		Cl	>100	>100
k		Cl	>100	>100

large substituents were synthesized to form hydrophobic interactions with the S<sub>3</sub> region. Table 2 shows the data for the initial set of compounds synthesized. The compounds contained P<sub>3</sub> amines with a terminal phenyl group that varied in the length of the carbon chain linker. The phenethyl analogue **24a** was the most potent of the series on TF/VIIa, but it showed no selectivity vs thrombin. The benzyl analogue **25b** was the first compound to show sub-micromolar activity on TF/VIIa along with 10-fold selectivity vs thrombin.

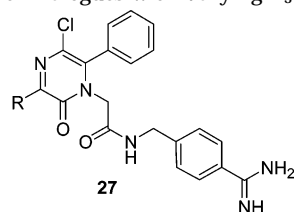
A series of compounds with substituted benzyl and phenethyl groups in the P<sub>3</sub> were prepared. A representative set is depicted in Table 3. Analogues with a P<sub>3</sub> benzyl group, regardless of substitution on the phenyl ring, showed selectivity vs thrombin, whereas analogues with a P<sub>3</sub> phenethyl group showed no selectivity vs thrombin. In fact, analogues with a P<sub>3</sub> phenethyl group,

**Table 2.** Pyrazinone Analogs with a P<sub>3</sub> Phenyl Ring Varying in the Length of the Carbon Chain Linker


compd	R	IC <sub>50</sub> (μM)	
		VIIa	IIa
<b>25a</b>	Ph	11.2	>30
<b>25b</b>	CH <sub>2</sub> Ph	0.77	7.63
<b>24a</b>	(CH <sub>2</sub> ) <sub>2</sub> Ph	0.63	0.16
<b>25c</b>	(CH <sub>2</sub> ) <sub>3</sub> Ph	12.6	23.6
<b>25d</b>	(CH <sub>2</sub> ) <sub>4</sub> Ph	4.1	7.1

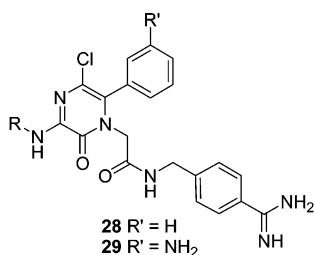
**Table 3.** Pyrazinone Analogs with a Substituted Benzyl or Phenethyl P<sub>3</sub> Substituent


compd	n	X	Y	IC <sub>50</sub> (μM)		
				VIIa	IIa	IIa/VIIa
<b>25b</b>	1	H	H	0.77	7.63	10
<b>26a</b>	1	<i>m</i> -CF <sub>3</sub>	H	6.3	18.9	3
<b>26b</b>	1	<i>p</i> -Cl	H	4.3	>30	>7
<b>26c</b>	1	3-F	6-F	3.8	>30	>7
<b>26d</b>	1	3-F	5-F	6	>30	>5
<b>24a</b>	2	H	H	0.63	0.16	0.24
<b>26e</b>	2	<i>m</i> -CF <sub>3</sub>	H	30	4.4	0.1
<b>26f</b>	2	<i>p</i> -Cl	H	0.6	<0.04	<0.07
<b>26g</b>	2	<i>m</i> -Cl	H	0.18	<0.04	<0.22

**Table 4.** Pyrazinone Analogues with Varying P<sub>3</sub> Substituents


Cpd	R	IC <sub>50</sub> (μM)	
		VIIa	IIa
<b>a</b>		6.3	20
<b>b</b>		>30	>30
<b>c</b>		9.1	19.9
<b>d</b>		6.4	8

regardless of substitution, were more potent on thrombin than on TF/VIIa.

**Table 5.** Pyrazinone Analogues with Varying P<sub>3</sub> Substituents

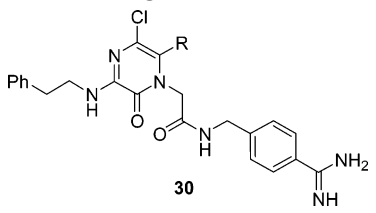
Cpd	R	IC <sub>50</sub> (μM)		Cpd	IC <sub>50</sub> (μM)		Cpd	R	IC <sub>50</sub> (μM)		Cpd	IC <sub>50</sub> (μM)	
		VIIa	IIa		VIIa	IIa			VIIa	IIa		VIIa	IIa
28				28			28						
a	CH <sub>3</sub>	0.7	20.4	a	0.06	>30	o		1.4	16.5	---	---	---
b	CH <sub>3</sub> CH <sub>2</sub>	0.4	11.3	b	0.04	28.4	p		3.0	15	---	---	---
c	CH <sub>3</sub> (CH <sub>2</sub> ) <sub>2</sub>	0.4	5.2	---	---	---	q		13	>30	---	---	---
d		0.7	8.7	---	---	---	r		0.50	20	---	---	---
e		0.72	3.0	---	---	---	s		0.88	10	g	0.14	>30
f	CH <sub>3</sub> (CH <sub>2</sub> ) <sub>3</sub>	3.2	27.9	c	0.1	17.85	t		0.50	10	h	0.09	>30
g		0.20	4.0	d	0.02	6.98	u		0.60	10	---	---	---
h		0.43	1.0	e	0.05	3.21	v		0.47	10	---	---	---
i		0.84	8.0	---	---	---	w		2.1	>30	---	---	---
j		1.8	2.1	---	---	---	x		20.9	>30	i	0.69	>30
k		0.9	1.2	---	---	---	y		8.0	37	---	---	---
l		9.8	5.2	---	---	---	z		0.89	13	---	---	---
m		0.40	4.6	f	0.02	8.0	aa		17.6	>30	---	---	---
n		1.0	10	---	---	---	bb		0.98	18.7	---	---	---

Several analogues with a tertiary P<sub>3</sub> amine were prepared (**27a–c**), all of which resulted in a loss of potency on TF/VIIa (Table 4). Replacing the P<sub>3</sub> nitrogen with a sulfur atom, as in **27d**, resulted in a decrease in potency. The P<sub>3</sub> NH hydrogen-bonds to Gly 216 of the peptide backbone in the S<sub>3</sub> pocket. As shown by this series of compounds, loss of this interaction results in a decrease in potency on TF/VIIa.

Table 5 contains analogues with alkyl, branched alkyl, and cyclic alkyl groups as the P<sub>3</sub> substituents (**28a–q**). With the exception of the analogues with larger cyclic alkyl groups, these compounds were consistently as active or more active than the benzyl analogues described above. The majority of the analogues with small alkyl and cyclic alkyl groups at P<sub>3</sub> (**28a–i**) had sub-micromolar potency with at least 10× selectivity vs thrombin. Also contained in Table 5 are analogues with

P<sub>3</sub> substituents possessing polar groups on the terminus (**28r–bb**). The polar analogues were comparable in activity to their alkyl analogues, with no significant increase in potency or selectivity.

Efforts to optimize the P<sub>2</sub> and P<sub>3</sub> regions of the inhibitor occurred simultaneously. It was shown that an aniline group in the P<sub>2</sub> region was significantly more active than the unsubstituted phenyl group. Thus, the more active P<sub>3</sub> analogues were synthesized with aniline in the P<sub>2</sub> (**29a–i**) and the activity compared with the data of the corresponding analogues with an unsubstituted phenyl group in the P<sub>2</sub> position (Table 5). The relative potency was analogous to that of the phenyl series. The majority of the compounds were approximately 10 times more active on TF/VIIa and significantly more selective over thrombin with the aniline in place of the unsubstituted phenyl in the P<sub>2</sub> position.

**Table 6.** Pyrazinone Analogues with Various P<sub>2</sub> Substituents


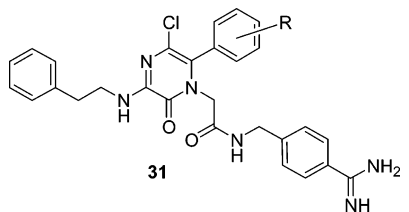
compd	R	IC <sub>50</sub> (μM)	
		VIIa	IIa
<b>30a</b>	Me	4.28	0.06
<b>30b</b>	Et	3.45	<0.04
<b>24a</b>	Ph	0.63	0.16
<b>30c</b>	Bn	> 30	4.0
<b>30d</b>	4-biphenyl	> 30	> 30

In general, the SAR studies indicate that the S<sub>3</sub> pocket of TF/VIIa prefers small alkyl groups for lipophilic interaction with Gln 217 and residues from the peptide segment 170E–170I (including Pro 170I). The NH is essential for potency as this hydrogen bonds to the Gly 216 of the peptide backbone.

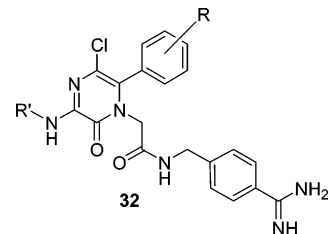
On the basis of crystal structure data, the S<sub>2</sub> pocket of TF/VIIa is relatively open and has a negative potential due to the presence of Asp 60. Among the coagulation proteases, only Factor VIIa has a negatively charged residue at position 60. Thrombin has a large insertion in the S<sub>2</sub> pocket with a number of aromatic amino acid residues. From the docking experiments, a benzyl group at P<sub>2</sub> seemed to occupy much of the space of the S<sub>2</sub> pocket. To confirm this, and to probe the depth of the S<sub>2</sub> pocket of TF/VIIa, scaffolds were synthesized from aldehydes containing R groups of various sizes. The data for a set of compounds with methyl, ethyl, phenyl, benzyl, and 4-biphenyl groups in the P<sub>2</sub> is shown in Table 6. This data set shows the phenyl group (**24a**) as the optimal size for fitting in the S<sub>2</sub> pocket. Larger groups, such as the benzyl (**30c**) and biphenyl (**30d**), showed no activity on TF/VIIa at 30 μM. Smaller groups, such as methyl (**30a**) and ethyl (**30b**), showed some TF/VIIa activity, but were more potent on thrombin. This is consistent with the difference in the S<sub>2</sub> pocket size of the two enzymes.

The next step was to determine whether substitution on the phenyl ring in the P<sub>2</sub> was tolerated and, if so, whether the size of the group or its position on the ring affected potency. A representative set of data for these studies is shown in Table 7. A variety of halogens and small alkyl groups could be placed in both the ortho and meta positions on the P<sub>2</sub> phenyl ring while maintaining potency vs TF/VIIa. However, activity on TF/VIIa decreased considerably when the group was in the para position. This trend held true when tested with a variety of groups in the P<sub>3</sub> position.

Having established an ortho- or meta-substituted phenyl as the optimal-sized P<sub>2</sub> group to occupy the S<sub>2</sub> region, the next objective was to determine which substituents gave the most active and selective TF/VIIa inhibitors. A variety of ortho- and meta-substituted P<sub>2</sub> phenyl analogues were prepared with a representative set shown in Table 8. Of particular interest is compound **29f**, with a *m*-amino group on the P<sub>2</sub> phenyl ring. It was theorized that since the S<sub>2</sub> pocket of TF/VIIa is larger in size than that of thrombin, and since Asp 60 is unique

**Table 7.** Pyrazinone Analogs with a Substituted P<sub>2</sub> Phenyl Ring


compd	R	IC <sub>50</sub> (μM)	
		VIIa	IIa
<b>24a</b>	H	0.63	0.16
<b>31a</b>	<i>o</i> -Cl	3.0	2.1
<b>31b</b>	<i>m</i> -Cl	1.98	0.72
<b>31c</b>	<i>p</i> -Cl	8.88	0.2
<b>31d</b>	<i>o</i> -F	1.8	1.2
<b>31e</b>	<i>m</i> -F	2.3	1.1
<b>31f</b>	<i>p</i> -F	8.1	0.1
<b>31g</b>	<i>o</i> -CF <sub>3</sub>	2.7	8.6
<b>31h</b>	<i>m</i> -CF <sub>3</sub>	2.9	3.5
<b>31i</b>	<i>p</i> -CF <sub>3</sub>	>30	6.3
<b>31j</b>	<i>o</i> -CH <sub>3</sub>	0.43	0.30
<b>31k</b>	<i>m</i> -CH <sub>3</sub>	1.0	0.89
<b>31l</b>	<i>p</i> -CH <sub>3</sub>	4.14	0.30
<b>31m</b>	<i>o</i> -OCH <sub>3</sub>	1.6	3.3
<b>31n</b>	<i>m</i> -OCH <sub>3</sub>	5.2	1.0
<b>31o</b>	<i>p</i> -OCH <sub>3</sub>	23.45	4.06

**Table 8.** Pyrazinone Analogs with a Substituted P<sub>2</sub> Phenyl Ring


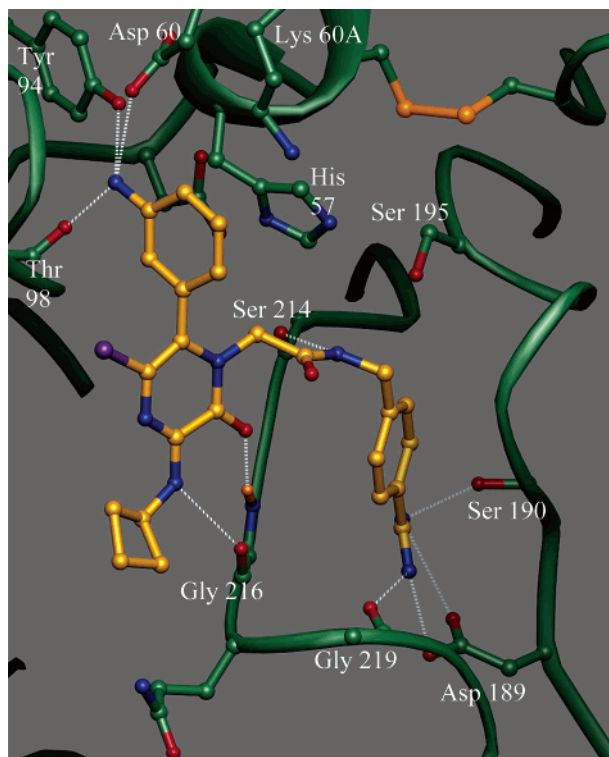
compd	R'	R	IC <sub>50</sub> (μM)	
			VIIa	IIa
<b>32a</b>	<i>c</i> Bu	<i>m</i> -bromo	4.2	> 30
<b>32b</b>	phenethyl	<i>m</i> -NO <sub>2</sub>	2.52	0.98
<b>32c</b>	phenethyl	<i>m</i> -NH <sub>2</sub>	0.07	0.9
<b>29d</b>	<i>i</i> Pr	<i>m</i> -NH <sub>2</sub>	0.02	6.98
<b>29f</b>	<i>c</i> Bu	<i>m</i> -NH <sub>2</sub>	0.02	8.0
<b>32d</b>	<i>c</i> Bu	<i>m</i> -OH	0.20	4.25
<b>32e</b>	<i>c</i> Bu	<i>o</i> -OH	0.34	> 30
<b>32f</b>	<i>i</i> Pr	<i>m</i> -CO <sub>2</sub> CH <sub>3</sub>	0.78	2.0
<b>32g</b>	<i>i</i> Pr	<i>m</i> -CO <sub>2</sub> H	0.36	2.8

to TF/VIIa, it would be possible to gain potency and achieve selectivity vs thrombin by placing a proton donor at the meta position of the P<sub>2</sub> phenyl ring. The *m*-amino analogue **29f** was prepared and resulted in a potent inhibitor on TF/VIIa (IC<sub>50</sub> = 20 nM) with increased selectivity against thrombin (400×) and Factor Xa (>5000×).

An X-ray crystal structure of compound **29f** bound to TF/VIIa is shown in Figure 4. It is very clear from the crystal structure that there is a four-centered hydrogen bonding interaction between the *m*-amino P<sub>2</sub> of **29f**, Asp 60, Tyr 94, and Thr 98. These key hydrogen bonding interactions with the S<sub>2</sub> pocket of TF/VIIa are likely responsible for the observed 20× boost in potency and the increase in selectivity vs thrombin over the unsubstituted P<sub>2</sub> phenyl analogue **28m**.

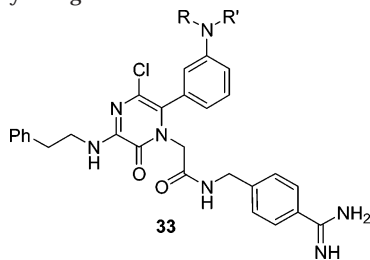
This theory was further confirmed by the data in Table 9, which shows a drop in potency when the aniline





**Figure 4.** Crystal structure of compound **29f** bound in the active site of TF/VIIa complex. The structure was refined to an  $R_{\text{free}}$  of 29.0% at 2.8 Å resolution. Some of the key side chains of Factor VIIa are displayed (C: green, N: dark blue, O: red, S: orange). The inhibitor is represented with carbon, nitrogen, oxygen, and chlorine atoms displayed in yellow, blue, red, and purple, respectively. The hydrogen bonds formed by the inhibitor are shown as dotted white lines. The *m*-amino group on the phenyl group of the inhibitor forms strong interactions with Asp 60, Tyr 94, and the carbonyl oxygen of Thr 98 in the  $S_2$  pocket.

**Table 9.** Pyrazinone Analogs with a Substituted  $P_2$  *m*-Aminophenyl Ring



**34**  
 TF/VIIa  $IC_{50}$  ( $\mu\text{M}$ ): 0.016  
 Thrombin  $IC_{50}$  ( $\mu\text{M}$ ): >100  
 Xa  $IC_{50}$  ( $\mu\text{M}$ ): >100

**Figure 5.** Pyrazinone intravenous POC compound **34**.

sible. Since the  $S_2$  pockets of the TF/VIIa and thrombin enzymes are substantially different, multiple substitution on the  $P_2$  *m*-aminophenyl ring should lead to increased selectivity over thrombin via additional interactions with the  $S_2$  pocket. Specifically, the Lys 60A residue was targeted as a potential site of interaction in the TF/VIIa  $S_2$  pocket. Compound **34** was prepared with a 3-amino-5-carboxyphenyl ring as the  $P_2$  substituent with the 5-carboxylic acid moiety intended to engage Lys 60A (Figure 5). The activity of **34** on TF/VIIa was relatively unchanged vs **29f**. However, the selectivity vs thrombin was dramatically increased from 400 $\times$  to > 6250 $\times$ . An X-ray crystal structure of **34** revealed that Lys 60A was engaged by the carboxyl moiety on  $P_2$ , which led to the superior selectivity profile for this compound (Figure 6). Compound **34** was deemed selective enough vs Factor Xa and thrombin to proceed with the preclinical intravenous proof-of-concept studies to demonstrate the separation between antithrombotic efficacy and bleeding side effects in a nonhuman primate model of electrolytic-induced arterial thrombosis.<sup>39</sup>

In conclusion, we used SBDD and multistep PASP library synthesis of pyrazinones to demonstrate that high levels of activity and selectivity for TF/VIIa are possible. Starting from a tripeptide- $\alpha$ -ketothiazole that was active on TF/VIIa, we were able to design a series of active and selective pyrazinone inhibitors of TF/VIIa that were reversible and did not capture the catalytic apparatus of the enzyme. These inhibitors exhibited sufficient levels of activity and selectivity for TF/VIIa vs Factor Xa and thrombin to proceed with our preclinical, intravenous proof-of-concept studies. These studies were designed to demonstrate the separation of antithrombotic efficacy and bleeding side effects in a nonhuman primate model of electrolytic-induced arterial thrombosis. Further efforts to refine the SAR in the pyrazinone series are in progress. In addition, a variety of core molecules as alternative central templates for the selective inhibition of TF/VIIa have been synthesized and will be reported in due course.

## Experimental Section

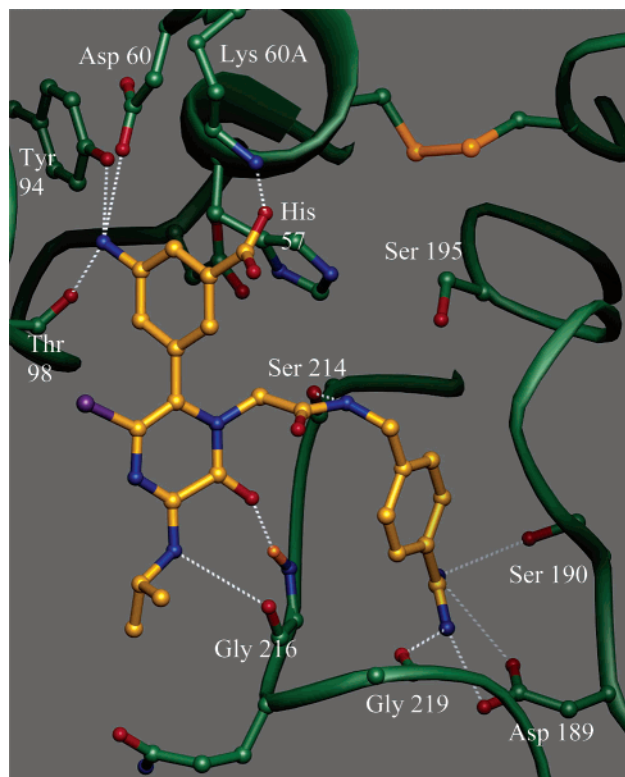
**General.** Solvents and chemicals were reagent grade or better and were obtained from commercial sources.  $^1\text{H}$  and  $^{13}\text{C}$  NMR spectra were recorded using a 300 or 400 MHz NMR spectrometer. Sample purities were determined by HPLC analysis equipped with a mass spectrometric detector using a C18 3.5  $\mu\text{m}$ , 30  $\times$  2.1 mm column, eluting with a gradient system of 5:95 to 95:5 acetonitrile:water with a buffer consisting of 0.1% TFA over 4.5 min at 1 mL/min and detected by DAD. HPLC purifications were conducted using a C18 15 mm, 100 Å, 25  $\times$  100 mm column, eluting with a gradient system of 5:95 to 95:5 acetonitrile:water with a buffer consisting of 0.1% TFA over 10 min at 30 mL/min, unless otherwise noted.

nitrogen was substituted with various groups. Functionalizing the  $P_2$  aniline nitrogen affects the key hydrogen bonding interactions with the  $S_2$  pocket.

Compound **29f** was sufficiently potent on TF/VIIa and selective enough on Factor Xa (>5000 $\times$ ) to proceed with the intravenous proof-of-concept studies. However, a more selective inhibitor vs thrombin was desired to unequivocally prove that separation between antithrombotic efficacy and bleeding side effects was pos-

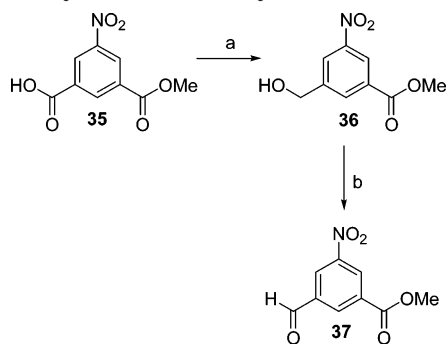
compd	R	R'	$IC_{50}$ ( $\mu\text{M}$ )	
			VIIa	IIa
<b>32c</b>	H	H	0.07	0.9
<b>33a</b>	CH <sub>3</sub>	H	0.60	0.58
<b>33b</b>	CH <sub>3</sub>	CH <sub>3</sub>	1.2	1.1
<b>33c</b>	COCH <sub>3</sub>	H	1.61	0.11
<b>33d</b>	COCF <sub>3</sub>	H	0.45	2.0
<b>33e</b>	SO <sub>2</sub> CH <sub>3</sub>	H	0.6	0.10





**Figure 6.** Crystal structure of compound **34** bound in the active site of TF/VIIa complex. The structure was refined to an  $R_{\text{free}}$  of 31.1% at 2.1 Å resolution. The atoms are colored as in Figure 4 with some of the key side chains of Factor VIIa shown. The hydrogen bonds formed by the inhibitor are shown as dotted white lines. Consistent with the structure of compound **29f**, the *m*-amino group forms close interactions in the  $S_2$  pocket. As predicted, the carboxylate group at the 5-position of the phenyl group forms interactions with the  $\epsilon$ -amino group of Lys 60A. The side chain of Lys 60A, which is on the surface, is disordered in most of the crystal structures of TF/VIIa complexes.

#### Scheme 5. Synthesis of Aldehyde **37**<sup>a</sup>



<sup>a</sup> Reagents: (a)  $\text{BH}_3$ , THF; (b)  $(\text{ClCO})_2$ , DMSO, TEA,  $\text{CH}_2\text{Cl}_2$ .

Yields were not optimized, with emphasis on purity of products rather than quantity. Recombinant soluble TF, consisting of amino acids 1–219 of the mature protein sequence, was expressed in *E. coli* and purified using a Mono Q Sepharose FPLC. Recombinant human VIIa was purchased from American Diagnostica, Greenwich, CT. Chromogenic substrate *N*-methylsulfonyl-D-Phe-Gly Arg-*p*-nitroaniline was prepared by American Peptide Company, Inc., Sunnyvale, CA. Factor Xa was obtained from Enzyme Research Laboratories, South Bend IN, thrombin from Calbiochem, La Jolla, CA, and trypsin and L-BAPNA from Sigma, St. Louis, MO. The chromogenic substrates S-2765 and S-2238 were purchased from Chromogenix, Sweden.

**PASP Library Synthesis. General Procedure A. Nucleophilic Displacement of 3-Chloropyrazinone **4** with Amine **5** to Afford Product **6**.** Individual reaction products were prepared in multiple reaction block vessels in a spatially addressed format. The desired dichloropyrazinone scaffold **4** (1.5 mL of a 0.2 M solution) in acetonitrile was added to the reaction vessels followed by a 3-fold stoichiometric excess of the amine **5** (4.5 mL of a 0.2 M solution) in acetonitrile. The reaction mixtures were incubated at 70 °C for 16–20 h. After being cooled to ambient temperature, the contents of each reaction vessel were taken on to the next step without purification.

**General Procedure B. Hydrolysis of the Benzyl Ester **6** to Afford Product **7**.** Each reaction vessel was charged with methanol (3 mL) and a 3–4-fold stoichiometric excess of aqueous potassium hydroxide (2.1 mL of a 0.5 M solution). The reaction block was shaken vertically for 3 h on an orbital shaker at ambient temperature. The contents of each reaction vessel were acidified with 0.3 mL of 12 M aqueous hydrochloric acid. Each reaction vessel was then opened, and the solutions were evaporated to dryness under nitrogen and/or a Savant apparatus. Alternatively, when the  $P_2$  phenyl ring contained an ester functionality, the pyrazinone **6** was treated with 10% palladium on carbon in methanol (2–4 mL) under 10 psi of hydrogen for 16–20 h to remove the benzyl ester. Polyamine resin **8** (1.5 g, ~4.2 mmol, 10–15-fold stoichiometric excess) was added to the solid carboxylic acid **7** followed by dichloromethane (12 mL) and water (1.2 mL). The mixture was shaken laterally for 6 h on an orbital shaker at ambient temperature (rotating the vials at least once so each side of the vial was agitated for a minimum of 2 h). The desired product **7** was sequestered away from the reaction byproducts and excess reactants as the insoluble adduct **9**. Simple filtration of the insoluble resin-adduct **9** and rinsing of the resin cake with dimethylformamide (3 × 3 mL), dichloromethane (3 × 3 mL), methanol (3 × 3 mL), and dichloromethane (3 × 3 mL) afforded the desired resin-bound product **9**. After drying the resin under vacuum for 2 h, an excess of hydrochloric acid in 1,4-dioxane (4.0 N, 8 mL) (7–8-fold stoichiometric excess based on the loading of amine functionality) along with dichloromethane (3 mL) was added to each reaction vessel to cleave the desired product **7** from the resin. The reaction block was shaken laterally for 2–20 h on an orbital shaker at ambient temperature. Simple filtration of the solution, rinsing of the resin cake with dimethylformamide/dichloromethane, and evaporation of the solvents afforded the desired products **7** in purified form, which were weighed and analyzed by LC/MS.

**General Procedure C. Coupling of Carboxylic Acids **7** with  $P_1$  Amine Inputs to Afford Product **10**.** The acid **7** was added as a solution in dichloromethane (3 mL) and dimethylformamide (2 mL) to each reaction vessel. A solution of hydroxybenzotriazole **12** (2 mg, 0.015 mmol, >0.05 equiv) in dimethylformamide/dichloromethane was added to each reaction vessel, followed by the polymer-bound carbodiimide reagent **11** (1.2–1.5-fold stoichiometric excess). The parallel reaction block was agitated vertically on an orbital shaker for 30 min to 1 h. The amine **14** (1 equiv) in dimethylformamide (0.10 mM), along with a 3-fold stoichiometric excess of *N*-methylmorpholine, if the amine **14** was a salt, was added to the activated acid **13** of each vessel. The parallel reaction block was then agitated vertically on an orbital shaker for 1–20 h at ambient temperature. An excess of the polyamine resin **8** (250 mg, ~0.7 mmol) and aldehyde resin **15** (100 mg, ~0.3 mmol), along with dichloromethane (1–3 mL), as needed for effective agitation, were added to each reaction vessel. The resin-charged reaction block was shaken vertically for 2 h on an orbital shaker at ambient temperature. Filtration of the insoluble resins and resin adducts, subsequent rinsing of the vessel resin-bed with dimethylformamide (3 × 1 mL), and concentration of the filtrates afforded pure products **10**, which were weighed and analyzed by LC/MS.

**General Procedure D. Deprotection of the BOC Group from Compounds **10** to Afford Products **21**.** For those

amines **14** which contained a BOC protecting group, hydrochloric acid in 1,4-dioxane (4.0 N, 3 mL) was added to the BOC protected compound **10** (~0.3 mmol) in a reaction vessel, and the solution was agitated on an orbital shaker at room temperature for 3 h. Evaporation of the solvents afforded the products **21**. If necessary, the products were purified by reverse-phase HPLC.

**General Procedure E. Deprotection of the CBz Group from Compounds 16 Using TMSI to Afford Products 21.** The residues **16** were dissolved in acetonitrile (1.5 mL). Sodium iodide and trimethylsilyl chloride (5-fold stoichiometric excess of each) were added, and the reaction mixtures were agitated vertically at 55 °C for 14–20 h. After being cooled to room temperature, the reactions were quenched with 0.1 mL of methanol. Poly(4-vinylpyridine) or *N,N*-(dimethyl)aminomethylpolystyrene resin (10-fold stoichiometric excess based on the amount of trimethylsilyl chloride and sodium iodide added) was added to each vessel to sequester the byproduct **22**. The mixtures were agitated for another 3 h and then filtered through Celite and rinsed with acetonitrile to remove byproduct **20** and the polymer-bound byproduct **22**. The filtrate was concentrated to afford products **21**. If necessary, the products were purified by reverse-phase HPLC.

**General Procedure F. Removal of CBz Protecting Group of Products 16 Using Pd/C to Afford Products 21.** The residues **16** were dissolved in methanol (2–4 mL). A catalytic amount of 10% Pd/C was added, and the reaction mixtures were stirred under 10 psi of hydrogen for 16–20 h. The mixtures were filtered through Celite, rinsed with methanol, and concentrated to afford pure products **21**. If necessary, the products were purified by reverse-phase HPLC.

The progress of the synthesis during production was followed by LC/MS of the intermediates. The final products with LC/MS purities of less than 85% were purified by reverse-phase chromatography. All products were characterized by LC/MS and HRMS, with several characterized by proton NMR. Data for final compounds are tabulated in Table 10 in Supporting Information.

**Synthesis of Compound 34 (Scheme 5). Methyl 3-(Hydroxymethyl)-5-nitrobenzoate 36.** 3-(Methoxycarbonyl)-5-nitrobenzoic acid **35** (30 g, 133 mmol) in tetrahydrofuran (100 mL) was cooled to –10 °C in a glass reactor equipped with a reflux condenser and addition funnel. Borane–tetrahydrofuran (260 mL, 1 M BH<sub>3</sub>–THF) was added dropwise over 2 h. The reaction was slowly warmed to room temperature and then heated to 64 °C. The reaction was stirred at reflux for 15 min, at which time TLC analysis (20% ethyl acetate–hexane) indicated the reaction was complete. After being cooled to room temperature, the reaction was quenched with 8 mL of acetic acid:water (1:1) and then neutralized to pH 7 using aqueous saturated sodium bicarbonate. The volatiles were removed under reduced pressure, and the residue was diluted with ethyl acetate (500 mL). The solution was washed with water (1 × 300 mL) and then brine (1 × 300 mL). The organic phase was dried over magnesium sulfate and filtered, and the solvent was removed under reduced pressure to give 19.8 g (70%) of **36** as a yellow solid: <sup>1</sup>H NMR (300 MHz, CDCl<sub>3</sub>) δ 4.00 (s, 3H), 4.89 (s, 2H), 8.35 (s, 1H), 8.43 (s, 1H), 8.77 (s, 1H); LRMS *m/z* 212.0 (M<sup>+</sup> + H).

**Methyl 3-Formyl-5-nitrobenzoate 37 (Scheme 5).** Dichloromethane (200 mL) was cooled to –78 °C in a glass reactor equipped with an addition funnel. Oxalyl chloride (13.9 mL, 0.16 mol) was added in one portion. Dimethyl sulfoxide (18.9 mL) in dichloromethane (100 mL) was added dropwise over 1 h. Compound **36** (19.6 g, 93 mmol) in dichloromethane (200 mL) was added dropwise over 1.5 h. The reaction was stirred at –78 °C for 45 min. Triethylamine (74.2 mL, 0.53 mol) was added via addition funnel over 45 min, upon which time the reaction turned yellow and thick. TLC analysis indicated the reaction was complete. The reaction was quenched with aqueous potassium hydrogensulfate (600 mL of a 1 M solution). The organic phase was washed with aqueous saturated sodium bicarbonate (1 × 600 mL), water (1 × 600 mL), and brine (1 × 600 mL). The organic phase was dried over sodium sulfate,

and the volatiles were removed under reduced pressure to give an orange oil. The crude oil was purified on 1 kg of silica gel using ethyl acetate:hexanes (20:80, v/v, isocratic) as the eluent to afford 15.4 g (78%) of **37** as an off-white solid: <sup>1</sup>H NMR (300 MHz, CDCl<sub>3</sub>) δ 4.06 (s, 3H), 8.86–8.87 (m, 1H), 8.90–8.91 (m, 1H), 9.10–9.11 (m, 1H), 10.19 (s, 1H); LRMS *m/z* 210.0 (M<sup>+</sup> + H).

**Methyl 3-[1-[2-(Benzyloxy)-2-oxoethyl]-3,5-dichloro-6-oxo-1,6-dihydropyrazin-2-yl]-5-nitrobenzoate 4'.** A separatory funnel was charged with glycine benzyl ester hydrochloride **2** (14.1 g, 69.7 mmol) and diluted with ethyl acetate (200 mL). The solution was washed with 1:1 brine:aqueous saturated sodium carbonate (2 × 250 mL). The organic portion was dried over sodium sulfate, and the volatiles were removed under reduced pressure to give the free base of **2**. The free base in dichloromethane (200 mL) was added to a glass reactor, followed by the dropwise addition of **37** (14.6 g, 70 mmol) in dichloromethane (100 mL) over 30 min. With caution, trimethylsilyl cyanide (26.0 mL, 195 mmol) was added via syringe over 20 min. A slight exotherm of 4 °C was observed during the addition. The reaction was stirred for 16 h at room temperature. The volatiles were removed under reduced pressure. The residue was diluted with ethyl acetate (400 mL) and washed with water (1 × 250 mL) and brine (1 × 250 mL). The organic phase was dried over magnesium sulfate and filtered, and the solvent was removed under reduced pressure to afford the intermediate as a yellow oil. The intermediate was dissolved in chlorobenzene (150 mL) and added dropwise over 1 h to a stirring, 50 °C solution of oxalyl chloride (24.3 mL, 279 mmol) in chlorobenzene (150 mL). The reaction was warmed to 80 °C and stirred for 16 h. The reaction was quenched with methanol (250 mL), and the volatiles were removed under reduced pressure to give crude **4'** as a brown oil: <sup>1</sup>H NMR (300 MHz, CDCl<sub>3</sub>) δ 4.03 (s, 3H), 4.39–4.66 (ABq, 2H, *J* = 17.0 Hz), 5.16 (d, 2H, *J* = 3.6 Hz), 7.21–7.25 (m, 2H), 7.28–7.35 (m, 3H), 8.35–8.36 (m, 1H), 8.41–8.42 (m, 1H), 8.98–8.99 (m, 1H); LRMS *m/z* 514.0 (M<sup>+</sup> + Na).

**Methyl 3-[1-[2-(Benzyloxy)-2-oxoethyl]-3-chloro-5-(isopropylamino)-6-oxo-1,6-dihydropyrazin-2-yl]-5-nitrobenzoate 6'.** Isopropylamine (11.9 mL, 140 mmol) was added to a stirring solution of crude **4'** (17.2 g, 35 mmol) in ethyl acetate (300 mL). The reaction turned black and was stirred at 55 °C for 16 h. The reaction mixture was filtered through Celite 545, and the volatiles were removed under reduced pressure. The crude residue was purified on 500 g of silica gel using ethyl acetate:hexanes (20:80, v/v, isocratic) as the eluent to afford 8.4 g (46%) of **6'** as a brown solid: <sup>1</sup>H NMR (300 MHz, CDCl<sub>3</sub>) δ 1.32 (d, 6H, *J* = 6.6 Hz), 4.01 (s, 3H), 4.21–4.33 (m, 1H), 4.32–4.58 (ABq, 2H, *J* = 17.0 Hz), 5.14 (d, 2H, *J* = 0.9 Hz), 7.21–7.39 (m, 5H), 8.33–8.34 (m, 1H), 8.38–8.39 (m, 1H), 8.90–8.91 (m, 1H); LRMS *m/z* 515.2 (M<sup>+</sup> + H).

**[6-[3-Amino-5-(methoxycarbonyl)phenyl]-5-chloro-3-(isopropylamino)-2-oxopyrazin-1(2H)-yl]acetic Acid 7'.** To a glass reactor were added **6'** (8.4 g, 16 mmol), 200 mL of methanol, and hydrochloric acid (7.5 mL of a 3 M methanolic solution). Under a blanket of nitrogen, 10% palladium on carbon (0.8 g, 10 wt %) was carefully added in a methanol slurry to the stirring solution. The vessel was sealed, purged of its atmosphere, and flushed with nitrogen 3× and then purged of its atmosphere and flushed with hydrogen 3×. The reaction was stirred at room temperature under a balloon of hydrogen for 16 h. The reaction was filtered through Celite 545, the volatiles were removed under reduced pressure, and the residue was diluted with ethyl acetate (300 mL). The organic phase was extracted with aqueous saturated sodium bicarbonate (2 × 300 mL). The aqueous phase was acidified to pH 4 with 1 M aqueous potassium hydrogensulfate and then extracted with ethyl acetate (3 × 350 mL). The organic phase was dried over magnesium sulfate and filtered, and the solvent was removed under reduced pressure to give 4.1 g (76%) of **7'** as an orange solid: <sup>1</sup>H NMR (300 MHz, CD<sub>3</sub>OD) δ 1.30 (d, 6H, *J* = 6.9 Hz), 3.89 (s, 3H), 4.16–4.24 (m, 1H), 4.38–4.39 (m, 2H), 6.83 (s, 1H), 7.20 (s, 1H), 7.43 (s, 1H); LRMS *m/z* 395.1 (M<sup>+</sup> + H).



**Methyl 3-Amino-5-[1-(2-{[4-((Z)-amino{[(benzyloxy)-carbonyl]imino}methyl)benzyl]amino}-2-oxoethyl)-3-chloro-5-(isopropylamino)-6-oxo-1,6-dihydropyrazin-2-yl]benzoate 10'.** To a glass bottle was added 7' (4.0 g, 10 mmol), hydroxybenzotriazole (0.41 g, 3 mmol), dichloromethane (40 mL), and dimethylformamide (5 mL). *N*-methylmorpholine (6.7 mL, 61 mmol) and benzyl amino[4-(aminomethyl)phenyl]methylencarbamate (3.6 g, 10 mmol) in dimethylformamide (15 mL) were added, followed by addition of the polymer-bound carbodiimide **11** (19.0 g, 18 mmol). The reaction was agitated on an orbital shaker for 3 h. Polyamine resin **8** (10.8 g, 30 mmol), aldehyde resin **15** (10.6 g, 30 mmol), and dichloromethane (20 mL) were added to the bottle, and the mixture was agitated for 1 h. The insoluble resins and resin adducts were filtered, and the resin cake was rinsed with dimethylformamide (2 × 50 mL) and dichloromethane (2 × 50 mL). Concentration of the filtrate afforded 5.3 g (79%) of **10'** as an orange solid: <sup>1</sup>H NMR (300 MHz, CDCl<sub>3</sub>) δ 1.23 (d, 6H, *J* = 6.6 Hz), 3.78 (s, 3H), 4.10–4.15 (m, 1H), 4.20 (s, 2H), 4.27–4.59 (ABq, 2H, *J* = 15.9 Hz), 5.16 (s, 2H), 7.03–7.76 (m, 12H); LRMS *m/z* 660.3 (M<sup>+</sup> + H).

**3-Amino-5-[1-(2-{[4-[amino(imino)methyl]benzyl]-amino)-2-oxoethyl]-3-chloro-5-(isopropylamino)-6-oxo-1,6-dihydropyrazin-2-yl]benzoic Acid 34.** Lithium hydroxide monohydrate (1.64 g, 39 mmol) in water (15 mL) was added to **10'** (5.3 g, 8 mmol) in methanol (100 mL). After stirring at room temperature for 16 h, the reaction was neutralized to pH 7 with 3 M aqueous hydrochloric acid. The volatiles were removed under reduced pressure, and the crude residue was purified by reverse-phase HPLC using a gradient of acetonitrile:water (0.1% TFA) (1:99 to 60:40) as the eluent to afford 1.8 g (34%) of **34** as an off-white solid: <sup>1</sup>H NMR (300 MHz, CD<sub>3</sub>OD) δ 1.31 (d, 6H, *J* = 6.6 Hz), 4.18–4.26 (m, 1H), 4.31–4.63 (m, 4H), 7.46–7.49 (m, 2H), 7.71–7.78 (m, 3H), 8.12–8.19 (m, 2H); HRMS (M + H): Calcd for C<sub>24</sub>H<sub>27</sub>ClN<sub>7</sub>O<sub>4</sub>: 512.1813; Found: 512.1819.

**Assays for Biological Activity. TF-VIIa Assay.** Recombinant soluble tissue factor (100 nM) and recombinant human Factor VIIa (2 nM) were added to a 96-well assay plate containing 0.4 mM of the substrate, *N*-methylsulfonyl-D-phenyl arg-*p*-nitroaniline and either inhibitor or buffer (5 mM CaCl<sub>2</sub>, 50 mM Tris-HCl, pH 8.0, 100 mM NaCl, 0.1% BSA). The reaction, in a final volume of 100 μL, was measured immediately at 405 nm to determine background absorbance. The plate was incubated at room temperature for 60 min, at which time the rate of hydrolysis of the substrate was measured by monitoring the reaction at 405 nm for the release of *p*-nitroaniline. All compounds were assayed in duplicate at seven concentrations. Percent inhibition at each concentration was calculated from OD<sub>405 nm</sub> value from the experimental and control sample. IC<sub>50</sub> values were calculated from a four-parameter logistic regression equation. For each compound the individual IC<sub>50</sub> values were within 10% of each other. The reported IC<sub>50</sub> represents an average of the duplicates.

**Xa Assay.** Human Factor Xa (0.3 nM) and *N*-α-benzyloxy-carbonyl-D-arginyl-L-glycyl-L-arginine-*p*-nitroaniline-dihydrochloride (S-2765) (0.15 mM) were added to a 96-well assay plate containing either inhibitor or buffer (50 mM Tris-HCl, pH 8.0, 100 mM NaCl, 0.1% BSA). The reaction, in a final volume of 100 μL, was measured immediately at 405 nm to determine background absorbance. The plate was incubated at room temperature for 60 min, at which time the rate of hydrolysis of the substrate was measured by monitoring the reaction at 405 nm for the release of *p*-nitroaniline. All compounds were assayed in duplicate at seven concentrations. Percent inhibition at each concentration was calculated from OD<sub>405 nm</sub> value from the experimental and control sample. IC<sub>50</sub> values were calculated from a four-parameter logistic regression equation. For each compound the individual IC<sub>50</sub> values were within 10% of each other. The reported IC<sub>50</sub> represents an average of the duplicates.

**Thrombin Assay.** Human thrombin (0.28 nM) and *H*-D-phenylalanyl-L-pipecolyl-L-arginine-*p*-nitroaniline dihydrochloride (0.06 mM) were added to a 96-well assay plate containing

either inhibitor or buffer (50 mM Tris-HCl, pH 8.0, 100 mM NaCl, 0.1% BSA). The reaction, in a final volume of 100 μL, was measured immediately at 405 nm to determine background absorbance. The plate was incubated at room temperature for 60 min, at which time the rate of hydrolysis of the substrate was measured by monitoring the reaction at 405 nm for the release of *p*-nitroaniline. All compounds were assayed in duplicate at seven concentrations. Percent inhibition at each concentration was calculated from OD<sub>405 nm</sub> value from the experimental and control sample. IC<sub>50</sub> values were calculated from a four-parameter logistic regression equation. For each compound the individual IC<sub>50</sub> values were within 10% of each other. The reported IC<sub>50</sub> represents an average of the duplicates.

**Crystal Structure.** Crystals of TF/VIIa complex were obtained by slight modification of the procedure described by Banner et al.<sup>46</sup>

**Acknowledgment.** The authors wish to thank James P. Doom, David Masters-Moore, and Ralph C. Scheibel for HRMS analysis, and Martin P. McGrath for running the hydrogenations. Diffraction data for the TF-VIIa complex with the pyrazinone inhibitors were collected at beamline 17-ID in the facilities of the Industrial Macromolecular Crystallography Association Collaborative Access Team (IMCA-CAT) at the Advanced Photon Source. IMCA-CAT facilities are supported by the corporate members of the IMCA and through a contract with Illinois Institute of Technology (IIT), executed through the IIT's Center for Synchrotron Radiation Research and Instrumentation. Use of the Advanced Photon Source was supported by the U.S. Department of Energy, Basic Energy Sciences, Office of Science, under Contract No. W-31-109-Eng-38.

**Supporting Information Available:** A table of characterization data of final pyrazinone products. This material is available free of charge via the Internet at <http://pubs.acs.org>.

## References

- Houston, D. S. Tissue Factor – a therapeutic target for thrombotic disorders. *Expert Opin. Ther. Targets* **2002**, *6*, 159–174.
- Golino, P. The inhibitors of the tissue Factor: Factor VII pathway. *Thromb. Res.* **2002**, *106*, V257–V265.
- Bajaj, M. S.; Birktoft, J. J.; Steer, S. A.; Bajaj, S. P. Structure and biology of tissue factor pathway inhibitor. *Thromb. Haemost.* **2001**, *86*, 959–972.
- Kaiser, B.; Hoppensteadt, D. A.; Fareed, J. Tissue factor pathway inhibitor: an update of potential implications in the treatment of cardiovascular disorders. *Expert Opin. Invest. Drugs* **2001**, *10*, 1925–1935.
- Girard, T. J.; Nicholson, N. S. The role of tissue Factor/Factor VIIa in the pathophysiology of acute thrombotic formation. *Curr. Opin. Pharmacol.* **2001**, *1*, 159–163.
- Coughlin, S. R. Thrombin signaling and protease-activated receptors. *Nature* **2000**, *407*, 258–264.
- Girard, T. J. Tissue Factor Pathway Inhibitor. In *New Therapeutic Agents in Thrombosis and Thrombolysis*; Sasahara, A. A., and Loscalzo, J., Eds.; Marcel Dekker: New York, 1998.
- Banner, D. W. The Factor VIIa/tissue Factor complex. *Thromb. Haemost.* **1997**, *78*, 512–515.
- Kirchhofer, D.; Nemerson, Y. Initiation of blood coagulation: the tissue Factor/Factor VIIa complex. *Curr. Opin. Chem. Biotech.* **1996**, *7*, 386–391.
- Petersen, L. C.; Valentin, S.; Hedner, U. Regulation of the extrinsic pathway system in health and disease: the role of Factor VIIa and tissue factor pathway inhibitor. *Thromb. Res.* **1995**, *79*, 1–47.
- Moreno P. R.; Bernardi, V. H.; Lopez-Cuellar, J.; Murcia, A. M.; Palacios, I. F.; Gold, H. K.; Mehran, R.; Sharma, S. K.; Nemerson, Y.; Fuster, V.; Fallon, J. T. Macrophages, smooth muscle cells, and tissue factor in unstable angina: implications for cell-mediated thrombogenicity in acute coronary syndromes. *Circulation* **1996**, *94*, 3090–3097.
- Edgington, T. S.; Mackman, N.; Brand, K.; Ruf, W. The structural biology of expression and function of tissue factor. *Thromb. Haemost.* **1991**, *66*, 67–79.

- (13) Sanderson, P. E. J. Anticoagulants: Inhibitors of thrombin and Factor Xa. *Annu. Rep. Med. Chem.* **2001**, *36*, 79–88.
- (14) Betz, A. Recent advances in Factor Xa inhibitors. *Expert Opin. Ther. Pat.* **2001**, *11*, 1007–1017.
- (15) Zhu, B. Y.; Scarborough, R. M. Factor Xa inhibitors: Recent advances in anticoagulant agents. *Annu. Rep. Med. Chem.* **2000**, *35*, 83–102.
- (16) Vacca, J. P. New Advances in the discovery of Thrombin and Factor Xa inhibitors. *Curr. Opin. Chem. Biol.* **2000**, *4*, 394–400.
- (17) Sanderson, P. E. J. Small, noncovalent serine protease inhibitors. *Med. Res. Rev.* **1999**, *19*, 179–197.
- (18) Ewing, W. R.; Pauls, H. W.; Spada, A. P. Progress in the design of inhibitors of coagulation Factor Xa. *Drugs Future* **1999**, *24*, 771–787.
- (19) Carroll, A. R.; Pierens, G. K.; Fechner, G.; de Almeida Leone, P.; Ngo, A.; Simpson, M.; Hyde, E.; Hooper, J. N. A.; Boström, S.-L.; Musil, D.; Quinn, R. J. Dysynsin A: A novel inhibitor of Factor VIIa and thrombin from a new genus and species of Australian sponge of the family Dysideidae. *J. Am. Chem. Soc.* **2002**, *124*, 13340–13341.
- (20) Hanessian, S.; Margarita, R.; Hall, A.; Johnstone, S.; Tremblay, M.; Parlanti, L. Total synthesis and structural confirmation of the marine natural product Dysynsin A: A novel inhibitor of thrombin and Factor VIIa. *J. Am. Chem. Soc.* **2002**, *124*, 13342–13343.
- (21) Hanessian, S.; Therrien, E.; Granberg, K.; Nilsson, I. Targeting thrombin and Factor VIIa: design, synthesis, and inhibitory activity of functionally relevant indolizidinones. *Bioorg. Med. Chem. Lett.* **2002**, *12*, 2907–2911.
- (22) Young, W. B.; Kolesnikov, A.; Rai, R.; Sprengeler, P. A.; Leahy, E. M.; Shrader, W. D.; Sangalang, J.; Burgess-Henry, J.; Spencer, J.; Elrod, K.; Cregar, L. Optimization of a screening lead for Factor VIIa/TF. *Bioorg. Med. Chem. Lett.* **2001**, *11*, 2253–2256.
- (23) Kohrt, J. T.; Filipinski, K. J.; Rapundalo, S. T.; Cody, W. L.; Edmunds, J. J. An efficient synthesis of 2-[3-(4-amidinophenyl-carbamoyl)naphthalen-2-yl]-5-[(2,2-methylpropyl)carbamoyl]benzoic acid: a Factor VIIa inhibitor discovered by the Ono Pharmaceutical Company. *Tetrahedron Lett.* **2000**, *41*, 6041–6044.
- (24) Jakobsen, P.; Horneman, A. M.; Persson, E. Inhibitors of the tissue Factor/Factor VIIa-induced coagulation: synthesis and in vitro evaluation of novel 2-aryl substituted pyrido[3,4-d]-[1,3]-, pyrido[2,3-d][1,3]-, pyrazino[2,3-d][1,3]-, pyrimido[4,5-d]-[1,3]-, pyrazolo[3,4-d][1,3]-, thieno[3,2-d][1,3]- and thieno[2,3-d]-[1,3]-oxazin-4-ones. *Bioorg. Med. Chem.* **2000**, *8*, 2803–2812.
- (25) Jakobsen, P.; Riitsmar Pedersen, B.; Persson, E. Inhibitors of the tissue Factor/Factor VIIa-induced coagulation: synthesis and in vitro evaluation of novel specific 2-aryl substituted 4H-3,1-benzoxazin-4-ones. *Bioorg. Med. Chem.* **2000**, *8*, 2095–2103.
- (26) Roussel, P.; Bradley, M.; Kane, P.; Bailey, C.; Arnold, R.; Cross, A. Inhibition of the tissue Factor/Factor VIIa complex: lead optimization using combinatorial chemistry. *Tetrahedron* **1999**, *55*, 6219–6230.
- (27) Gallagher, K. P.; Mertz, T. E.; Chi, L.; Rubin, J. R.; Uprichard, A. C. G. Inhibitors of tissue Factor/Factor VIIa. *Handbook Exp. Pharmacol.* **1999**, *132*, 421–445.
- (28) Wang, D.; Girard, T. J.; Kasten, T. P.; LaChance, R. M.; Miller-Wideman, M. A.; Durley, R. C. Inhibitory activity of unsaturated fatty acids and anaradic acids toward soluble tissue Factor-Factor VIIa complex. *J. Nat. Prod.* **1998**, *61*, 1352–1355.
- (29) Semple, J. E.; Rowley, D. C.; Brunck, T. K.; Ripka, W. C. Synthesis and biological activity of P2–P4 azapeptidomimetic P1-argininal and P1-ketoargininamide derivatives: a novel class of serine protease inhibitors. *Bioorg. Med. Chem. Lett.* **1997**, *7*, 315–320.
- (30) Uchiba, M.; Okajima, K.; Abe, H.; Okabe, H.; Takatsuki, K. Effect of nafamostat mesylate, a synthetic protease inhibitor, on tissue Factor-Factor VIIa complex activity. *Thromb. Res.* **1994**, *74*, 155–161.
- (31) Butenas, S.; Ribarik, N.; Mann, K. G. Synthetic substrates for human Factor VIIa and Factor VIIa-tissue Factor. *Biochemistry* **1993**, *32*, 6531–6438.
- (32) Van der Woerd-De Lange, J. A.; Van Dam-Mieras, M. C. E.; Hemker, H. C. Inhibition of activated Factors II, VII, IX, and X by synthetic organic compounds directed against the active-site seryl residue. *Haemostasis* **1981**, *10*, 315–47.
- (33) Szalony, J. A.; Taite, B. B.; Girard, T. J.; Nicholson, N. S.; Lachance, R. M. Pharmacological intervention at disparate sites in the coagulation cascade: Comparison of anti-thrombotic efficacy vs bleeding propensity in a rat model of acute arterial thrombosis. *J. Thromb. Thrombolysis* **2003**, *14*, 113–121.
- (34) Zoldhelyi, P.; McNatt, J.; Shelat, H. S.; Yamamoto, Y.; Chen, Z.-Q.; Willerson, J. T. Thromboresistance of balloon-injured porcine carotid arteries after local gene transfer of human tissue factor pathway inhibitor. *Circulation* **2000**, *101*, 289–295.
- (35) Himber, J.; Kirchhofer, D.; Riedereer, M.; Tschopp, T. B.; Steiner, B.; Roux, S. P. Dissociation of antithrombotic effect and bleeding time prolongation in rabbits by inhibiting tissue factor function. *Thromb. Haemost.* **1997**, *7*, 1142–1149.
- (36) Harker, L. A.; Hanson, S. R.; Wilcox, J. N.; Kelly, A. B. Antithrombotic and antilesion benefits without hemorrhagic risks by inhibiting tissue factor pathway. *Haemostasis* **1996**, *26* (suppl 1), 76–82.
- (37) South, M. S.; Dice, T. A.; Lachance, R. M.; Girard, T. J.; Stevens, A. M.; Stegeman, R. A.; Stallings, W. C.; Kurumbail, R. G.; Parlow, J. J. Polymer-assisted solution-phase (PASP) parallel synthesis of an  $\alpha$ -ketothiazole library as tissue Factor VIIa inhibitors. *Bioorg. Med. Chem. Lett.* **2003**, *13*, 2363–2367.
- (38) Parlow, J. J.; Dice, T. A.; Lachance, R. M.; Girard, T. J.; Stevens, A. M.; Stegeman, R. A.; Stallings, W. C.; Kurumbail, R. G.; South, M. S. Polymer-assisted solution-phase (PASP) parallel synthesis of an  $\alpha$ -ketothiazole library as tissue Factor VIIa inhibitors. *J. Med. Chem.* **2003**, *46*, 4043–4049.
- (39) Suleymanov, O. D.; Szalony, J. A.; Salyers, A. K.; Lachance, R. M.; Parlow, J. J.; South, M. S.; Wood, R. S.; Nicholson, N. S. Pharmacological interruption of acute thrombus formation with minimal hemorrhagic complications by a small molecule tissue Factor/Factor VIIa inhibitor: Comparison to Factor Xa and thrombin inhibition in a nonhuman primate thrombosis model. *J. Pharmacol. Exp. Ther.* **2003**, in press.
- (40) South, M. S.; Parlow, J. J.; Jones, D. E.; Case, B.; Dice, T.; Lindmark, R.; Hayes, M. J.; Rueppel, M. L.; Fenton, R.; Franklin, G. W.; Huang, H.-C.; Huang, W.; Kusturin, C.; Long, S. A.; Neumann, W. L.; Reitz, D.; Trujillo, J. I.; Wang, C.-C.; Wood, R.; Zeng, Q.; Mahoney, M. W. Preparation of arylpyrazinones as coagulation cascade serine protease inhibitors. WO 0187854, 2001.
- (41) South, M. S.; Parlow, J. J.; Jones, D. E.; Case, B.; Dice, T.; Lindmark, R.; Hayes, M. J.; Rueppel, M. L.; Fenton, R. K.; Franklin, G. W.; Huang, H.-C.; Huang, W.; Kusturin, C.; Long, S. A.; Neumann, W. L.; Reitz, D. B.; Trujillo, J. I.; Wang, C.-C.; Wood, R.; Zeng, Q. Preparation of arylpyrazinones as coagulation cascade serine protease inhibitors. WO 0069834 2000.
- (42) South, M. S.; Case, B. L.; Wood, R. S.; Jones, D. E.; Hayes, M. J.; Girard, T. J.; Lachance, R. M.; Nicholson, N. S.; Clare, M.; Stevens, A. M.; Stegeman, R. A.; Stallings, W. C.; Kurumbail, R. G.; Parlow, J. J. Structure-based drug design of pyrazinone antithrombotics as selective inhibitors of the tissue Factor VIIa complex. *Bioorg. Med. Chem. Lett.* **2003**, *13*, 2319–2325.
- (43) Kembal-Cook, G. J.; Daniel, J. D.; Tuddenham, E. G. D.; Harlos, K. Crystal structure of active site-inhibited human coagulation Factor VIIa (des-Gla). *J. Struct. Biol.* **1999**, *127*, 213–223.
- (44) Pike, A. C. W.; Brzozowski, A. M.; Roberts, S. M.; Olsen, O. H.; Persson, E. Structure of human Factor VIIa and its implications for the triggering of blood coagulation. *Proc. Natl. Acad. Sci. U. S. A.* **1999**, *96*, 8925–8930.
- (45) Perera, L.; Darden, T. A.; Pedersen, L. G. Probing the structural changes in the light chain of human coagulation Factor VIIa due to tissue factor association. *Biophys. J.* **1999**, *77*, 99–113.
- (46) Banner, D. W.; D'Arcy, A.; Chene, C.; Winkler, F. K.; Guha, A.; Konigsberg, W. H.; Nemerson, Y.; Kirchhofer, D. The crystal structure of the complex of blood coagulation Factor VIIa with soluble tissue factor. *Nature* **1996**, *380*, 41–46.
- (47) Tulinsky, A. Molecular Interactions of Thrombin. *Semin. Thromb. Hemost.* **1996**, 117–124.
- (48) Stubbs, M. T.; Bode, W. The clot thickens: clues provided by thrombin structure. *Trends Biochem. Sci.* **1995**, *20*, 23–28.
- (49) Adler, M.; Davey, D. D.; Phillips, G. B.; Kim, S. H.; Jancarik, J.; Rumennik, G.; Light, D. R.; Whitlow, M. Preparation, characterization, and the crystal structure of the inhibitor ZK-807834 (CI-1031) complexed with Factor Xa. *Biochemistry* **2000**, *39*, 12534–12542.
- (50) Maignan, S.; Guilloteau, J. P.; Pouzieux, S.; Choi-Sledeski, Y. M.; Becker, M. R.; Klein, S. I.; Ewing, W. R.; Pauls, H. W.; Spada, A. P.; Mikol, V. Crystal structures of human Factor Xa complexed with potent inhibitors. *J. Med. Chem.* **2000**, *43*, 3226–3232.
- (51) Kamata, K.; Kawamoto, H.; Honma, T.; Iwama, T.; Kim, S. H. Structural basis for chemical inhibition of human blood coagulation Factor Xa. *Proc. Natl. Acad. Sci. U. S. A.* **1998**, *95*, 6630–6635.
- (52) Padmanabhan, K.; Padmanabhan, K. P.; Tulinsky, A.; Park, C. H.; Bode, W.; Huber, R.; Blankenship, D. T.; Cardin, A. D.; Kisiel, W. Structure of human des(1–45) Factor Xa at 2.2 Å resolution. *J. Mol. Biol.* **1993**, *232*, 947–966.
- (53) Brandstetter, H.; Kuhne, A.; Bode, W.; Huber, R.; von der Saal, W.; Wirthensohn, K.; Engh, R. A. X-ray structure of active site-inhibited clotting Factor Xa. Implications for drug design and substrate recognition. *J. Biol. Chem.* **1996**, *271*, 29988–29992.
- (54) Burgey, C. S.; Robinson, K. A.; Lyle, T. A.; Sanderson, P. E. J.; Lewis, S. D.; Lucas, B. J.; Krueger, J. A.; Singh, R.; Miller-Stein, C.; White, R. B.; Wong, B.; Lyle, E. A.; W., Peter, D.; Coburn, C. A.; Dorsey, B. D.; Barrow, J. C.; Stranieri, M. T.; Holahan, M.



- A.; Sitko, G. R.; Cook, J. J.; McMasters, D. R.; McDonough, C. M.; Sanders, W. M.; Wallace, A. A.; Clayton, F. C.; Bohn, D.; Leonard, Y. M.; Detwiler, T. J., Jr.; Lynch, J. J., Jr.; Yan, Y.; Chen, Z.; Kuo, L.; Gardell, S. J.; Shafer, J. A.; Vacca, J. P. Metabolism-directed optimization of 3-aminopyrazinone acetamide thrombin inhibitors. Development of an orally bioavailable series containing P1 and P3 pyridines. *J. Med. Chem.* **2003**, *46*, 461–473.
- (55) Singh, R.; Silva Elipse, M. V.; Pearson, P. G.; Arison, B. H.; Wong, B. K.; White, R.; Yu, X. O.; Burgey, C. S.; Lin, J. H.; Baillie, T. A. Metabolic activation of a pyrazinone-containing thrombin inhibitor. evidence for novel biotransformation involving pyrazinone ring oxidation, rearrangement, and covalent binding to proteins. *Chem. Res. Toxicol.* **2003**, *16*, 198–207.
- (56) Sanderson, P. E. J.; Cutrona, K. J.; Dyer, D. L.; Krueger, J. A.; Kuo, L. C.; Lewis, S. D.; Lucas, B. J.; Yan, Y. Small, low nanomolar, noncovalent thrombin inhibitors lacking a group to fill the distal binding pocket. *Bioorg. Med. Chem. Lett.* **2003**, *13*, 161–164.
- (57) Reiner, J. E.; Siev, D. V.; Araldi, G.; Cui, J. J.; Ho, J. Z.; Reddy, K. M.; Mamedova, L.; Vu, P. H.; Lee, K. S.; Minami, N. K.; Gibson, T. S.; Anderson, S. M.; Bradbury, A. E.; Nolan, T. G.; Semple, J. E. Noncovalent thrombin inhibitors featuring P<sub>3</sub>-heterocycles with P<sub>1</sub>-monocyclic arginine surrogates. *Bioorg. Med. Chem. Lett.* **2002**, *12*, 1203–1208.
- (58) Sanderson, P. E. J.; Lyle, T. A.; Cutrona, K. J.; Dyer, D. L.; Dorsey, B. D.; McDonough, C. M.; Naylor-Olsen, A. M.; Chen, I.; Chen, Z.; Cook, J. J.; Cooper, C. M.; Gardell, S. J.; Hare, T. R.; Krueger, J. A.; Lewis, S. D.; Lin, J. H.; Lucas, B. J., Jr.; Lyle, E. A.; Lynch, J. J., Jr.; Stranieri, M. T.; Vastag, K.; Yan, Y.; Shafer, J. A.; Vacca, J. P. Efficacious, orally bioavailable thrombin inhibitors based on 3-aminopyridinone or 3-aminopyrazinone acetamide peptidomimetic templates. *J. Med. Chem.* **1998**, *41*, 4466–4474.
- (59) Vekemans, J.; Pollers-Wieers, C.; Hoornaert, G.; A new synthesis of substituted 2(1H)-pyrazinones. *J. Heterocycl. Chem.* **1983**, *20*, 919–923.
- (60) Gloanec, P.; Herve, Y.; Bremond, N.; Lecouve, J.; Breard, F.; De Nanteuil, G. Synthesis of benzyl (6S)-1,3-dichloro-4-oxo-4,6,7,8-tetrahydro-pyrrolo[1,2-a]pyrazine-6-carboxylic ester, a new conformationally constrained peptidomimetic derivative. *Tetrahedron Lett.* **2002**, *43*, 3499–3501.
- (61) Flynn, D. L.; Devraj, R. V.; Parlow, J. J. *Polymer-Assisted Solution-Phase Methods for Chemical Library Synthesis*; Burgess, K., Ed.; Solid-Phase Organic Synthesis; John Wiley & Sons: New York, 2000; Chapter 5.
- (62) Parlow, J. J.; Devraj, R. V.; South, M. S. Solution-phase chemical library synthesis using polymer-assisted purification techniques. *Curr. Opin. Chem. Biol.* **1999**, *3*, 320–336.
- (63) Flynn, D. L.; Devraj, R. V.; Naing, W.; Parlow, J. J.; Weidner, J. J.; Yang, S. Polymer-assisted solution phase (PASP) chemical library synthesis. *Med. Chem. Res.* **1998**, *8*, 219–243.
- (64) Ji, J.; Zhang, D.; Ye, Y.; Xing, Q. Studies on the reactions of HOBt, HOObt, HOSu with dichloroalkane solvents. *Tetrahedron Lett.* **1998**, *39*, 6515–6516.
- (65) South, M. S.; Dice, T. A.; Parlow, J. J. Polymer-assisted solution-phase (PASP) library synthesis of  $\alpha$ -ketoamides. *Biotechnol. Bioeng.* **2000**, *61*, 51–57.
- (66) Olah, G. A.; Narang, S. C.; Gupta, B. G. B.; Malhotra, R. Synthetic methods and reactions. 62. Transformations with chlorotrimethylsilane/sodium iodide, a convenient in situ iodotrimethylsilane reagent. *J. Org. Chem.* **1979**, *44*, 1247–1251.
- (67) The TF/VIIa enzyme potency for the 5-hydropyrazinones vs the corresponding 5-chloropyrazinone analogues are essentially equal with no more than a 2 $\times$  difference in IC<sub>50</sub> values.
- (68) A full detail of compounds with P<sub>1</sub> arginine mimetic amides will be the topic of a future publication.

JM030131L